



Appraisal of trace metals pollution, sources and associated health risks using the geochemical and multivariate statistical approach

Natarajan Rajmohan¹ · Milad H. Z. Masoud¹ · Burhan A. M. Niyazi^{1,2} · Abdulaziz M. Alqarawy^{1,2}

Received: 22 December 2022 / Accepted: 2 April 2023 / Published online: 15 April 2023
© The Author(s) 2023

Abstract

Trace metals pollution in the freshwater system is an emerging concern. Thus, a systematic study was performed in the Wadi Fatimah basin to appraise the trace metals pollution status, sources and associated health risks using integrated tools, namely indices, international standards, multivariate statistical techniques and health risk assessment models. The groundwater salinity shows a wide range (TDS = 391 to 11,240 mg/l). The heavy metal pollution index and contamination index justify that most of the samples are unfit for drinking due to high metal pollution. Severe pollution is noticed by the Li (100%), Ni (98%), Pb (86%) and B (78%), and it is in the decreasing order of Mo > Cr > Al > Fe = Mn > V > Sr > Ag > Cu. Pearson correlation matrix suggests that most of the metals have a significant strong positive correlation with Al, Fe and Mn and originated from geogenic sources. Principal components analysis and R-mode HCA indicate that trace metals are mostly derived from weathering of aluminium silicates, oxides/hydroxides of Fe and Mn followed by evaporation, evaporite dissolution and restricted flow. Q-mode HCA resulted in 4 clusters, and the water chemistry of WG1 and WG4 is governed by mineral weathering. In addition, evaporation also enriched the metal load and salinity in WG4 wells. In WG2, the water chemistry is predominantly affected by long storage, evaporation and mineral weathering. In WG3, the water chemistry is influenced by evaporation, irrigation return flow and evaporite dissolution. The hazard quotient and hazard index suggest that groundwater in this basin causes potential non-carcinogenic health risks to the consumer. This study strongly recommends treatment for groundwater before supply to the local inhabitants.

Keywords Groundwater pollution · Trace metals · Health risk assessment · Multivariate statistical analysis · Wadi Fatimah · Saudi Arabia

Introduction

Groundwater pollution due to trace metal accumulation is a serious concern worldwide as groundwater is an important source for various sectors, namely drinking, agriculture and industries. Recent studies give more importance to exploring the metals contamination, and their sources in groundwater because most of them are toxic even at low concentrations, persistent and non-biodegradable (Alfaifi et al. 2021; Long et al. 2021; Rajmohan et al. 2022). Further, polluted water resources act as a source for metal transfer/transport to the ecosystem and living organisms. Numerous studies were performed globally to evaluate the metal pollution status and sources in the groundwater (Prasanna et al. 2012; Palmucci et al. 2016; Arslan et al. 2017; Esmaeili et al. 2018; Barzegar et al. 2019; Mthembu et al. 2020; Usman et al. 2020; Rajmohan et al. 2022).

✉ Natarajan Rajmohan
rnatarajan@kau.edu.sa; nrmohan_2000@yahoo.com

Milad H. Z. Masoud
mhmasoud@kau.edu.sa

Burhan A. M. Niyazi
bniazi@kau.edu.sa

Abdulaziz M. Alqarawy
aalqaraawi@kau.edu.sa

¹ Water Research Center, King Abdulaziz University, Jeddah 21598, Saudi Arabia

² Faculty of Meteorology, Environment and Arid Land Agriculture, King Abdulaziz University, Jeddah 21598, Saudi Arabia

Metals enrichment in the aquifer occurred through geogenic and anthropogenic processes. Geogenic sources such as weathering of bedrock, volcanic emission, soil–water interaction, flushing of weathered materials and seawater invasion in coastal regions (Basahi et al. 2018; Wen et al. 2019; Rajmohan et al. 2022) and anthropogenic processes, namely industries, agriculture, mining, wastewater recharge, sewage lines leakage and dumping sites (Caritat et al. 1998; Nouri et al. 2008; Rajmohan et al. 2017; Samadder et al. 2017) are widely reported for the accumulation of metals in the aquifer.

In the Arabian Peninsula, water resources are limited and most of the countries in this region experience high water demand due to a lack of surface and groundwater resources and low rainfall, and high evaporation (Lezzaik and Milewski 2018). The Kingdom of Saudi Arabia (KSA) also experiences water scarcity owing to rapid growth in the agricultural sector, industries, population, and urbanization. In addition, groundwater contamination is also an emerging issue in this kingdom. Earlier studies documented the groundwater deterioration in this country and mostly occurred through natural sources and anthropogenic activities (Alshikh 2011; Al-Hobaib et al. 2013; Sharaf 2013; Zaidi et al. 2015; Bamousa and El Maghraby 2016; Rajmohan et al. 2019, 2021; Alqahtani et al. 2020; Alfaifi et al. 2021; Masoud et al. 2022). Further, some studies focused on metals accumulation in the groundwater in this region (Al-Hobaib et al. 2013; Basahi et al. 2018; Alfaifi et al. 2021; Alshehri et al. 2021; Rajmohan et al. 2022). These studies ensure that detailed knowledge of groundwater quality and pollution status is imperative for sustainable groundwater management.

The present study was performed in the Wadi Fatimah basin, Makkah Al-Mukarramah Province, Saudi Arabia. Rural communities in this basin rely on groundwater for domestic, livestock and agricultural activities. Earlier studies conducted in this basin reported groundwater deterioration (Alyamani 2007; Sharaf 2013; Alshehri et al. 2022; Osta et al. 2022) and most of them discussed on geology, hydrogeology and water suitability. None of them provided deep knowledge about the water chemistry and metal pollution in this basin. Hence, the present study can aid researchers to acquire insights about trace metals pollution status, sources and associated geochemical processes in the groundwater in Wadi Fatimah.

The primary goal of this study is to (a) appraise the extent of trace metals distribution in this aquifer, (b) evaluate the groundwater suitability for drinking using World Health Organisation (WHO) and United State Environmental Protection Agency (USEPA) prescribed drinking water standards, (c) assess the groundwater pollution status using heavy metal pollution index (HPI) and contamination index (Cd), (d) ascertain the trace metals source using the multivariate

statistical tool and (e) evaluate the health risks owing to exposure to trace metals for residents in this basin. This study renders a background knowledge about the trace metals distribution and status that will assist groundwater management and supply in this basin.

Study area

Wadi Fatimah basin is located in Makkah Al-Mukarramah Province and covers about 4869 km² (Fig. 1a). The study basin is a part of the Tihama coast of the Arabian shield and slopes towards the Red Sea. Wadi Fatimah basin is extending from the Taif water divide to the coast of the Red Sea. The annual average rainfall varies from 80 to 150 mm. In the upper reaches, it goes to 280 mm, whereas the lower reaches are dry and receive 80 mm (Alyamani and Hussein 1995; Şen et al. 2017; Osta et al. 2022). In this basin, vast variation is noticed in the climate and rainfall due to varying topography (Şen et al. 2017). Likewise, the maximum temperature ranges from 30 to 35 °C and the annual evaporation is > 1000 mm/year (Alyamani and Hussein 1995).

Geomorphologically, the Wadi Fatimah basin expresses typical characteristics of Saudi hydrographic basins in the western part of the escarpment ridge of the Arabian shield. It initiates from the eastern high mountainous range of sharp gradients and slopping towards the west at the coastal plain of the Tihama region (Alyamani and Hussein 1995; Hamimi et al. 2012). The elevation ranges between 10 and 2314 m in this basin.

Wadi Fatimah basin exhibits several geomorphological landscapes and is classified into three classes, namely the mountainous area, the hilly region and the piedmont plains. The mountainous area has high elevations (2300 m above mean sea level (AMSL)) and includes Proterozoic rocks, which form the water divide of the drainage basin. The hilly region is located in the eastern and middle portions of the basin that consists of undulating dissected and eroded rocks. The piedmont plains are between high lands and the Red sea and include morpho-tectonic depressions with a high order of the stream network.

Geologically, the Wadi Fatimah basin is comprised of Precambrian, Tertiary rocks, and Quaternary alluvial deposits (Fig. 1a) (Hamimi et al. 2012). The Precambrian basement rocks are composed of Proterozoic basalt to rhyolite (volcanic), metamorphic rocks and intercrossed with plutonic Gabbro and Diorite dykes. The exposures of tertiary rocks are encountered below the lava and Quaternary deposits by about 14% of the area of the Wadi Fatimah basin. These Tertiary rocks are sandstone, shale, and mudstones with conglomerates. Quaternary aquifer covers 22% of the Wadi Fatimah basin and its thickness ranges from 2 to 80 m, which consists of gravels, sands, alluvial, and Wadi deposits.

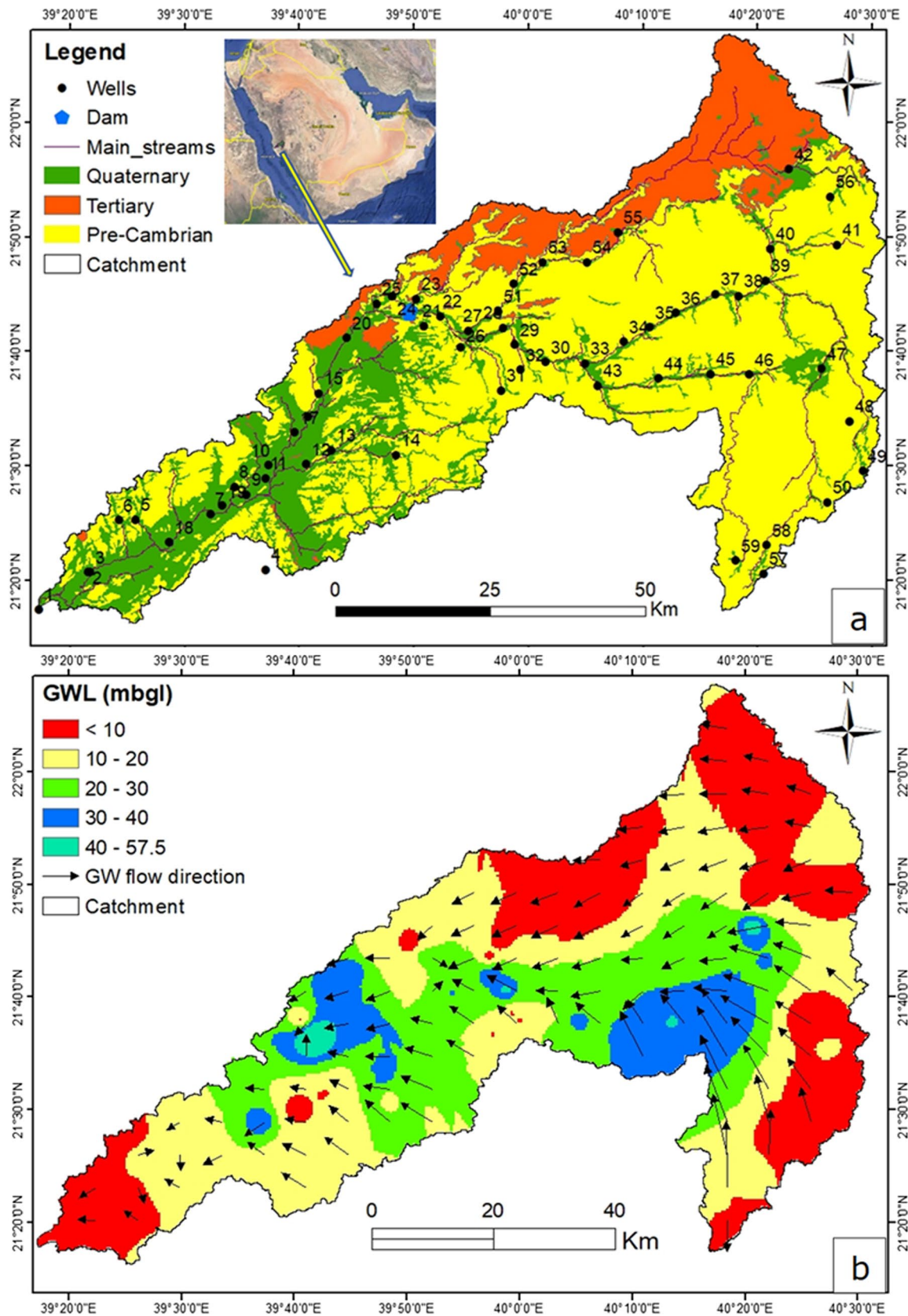


Fig. 1 Sampled wells location, geology and drainage pattern (a) and depth to groundwater level and groundwater flow direction (b) in the Wadi Fatimah basin

In the Quaternary aquifer, the hydraulic conductivity value is from 15 to 79 m/day with an average value of 43.9 m/day whereas the transmissivity value is between 150.3 and 2008 m²/day with a mean value of 1026 m²/day (Osta et al. 2022). This shallow aquifer is mostly recharged through flash floods and runoff events. The depth to groundwater level, measured in this study, varied from < 1 to 57.6 m and it is deeper in the central part of this basin (Fig. 1b). In this basin, the groundwater flows from the east and northeast to the southwest direction. Agriculture and horticulture are predominant groundwater consumers along with livestock in this basin.

Materials and methods

In total, 59 samples were obtained from both bore and dug wells in the Wadi Fatimah basin and their locations were recorded using a global position system (GPS, Garmin) (Fig. 1). Before pumping, groundwater levels were measured using a water level sounder. A portable handheld meter (SevenGo Duo SG23, Mettler Toledo) was used to measure the pH, electrical conductivity (EC), and temperature in the field. International standard protocols (APHA 2017) were employed during water sampling, handling, storage and chemical analysis. After the stabilization of EC and pH during pumping, water samples were collected in HDPE bottles (500 ml). Water samples were filtered (0.45 µm), acidified and stored at 4 °C and transported to the laboratory. Fifteen trace metals, namely Ag, Al, B, Ba, Cr, Cu, Fe, Li, Mn, Mo, Ni, Pb, Sr, V, and Zn, were analysed by inductively coupled plasma atomic emission spectrometry (ICP-AES, Shimadzu ICPE-9000). ICP-AES was calibrated by Accu Trace Reference Standard and Accu Trace Blank. Both standard and blank were run frequently to ensure the precision and accuracy of the analyses. The detection limit for the metals is 1 µg/l except for Mo (10 µg/l) and Al (10 µg/l).

Groundwater quality data were employed to perform multivariate statistical analysis and to calculate the contamination index (C_d) and heavy metal pollution index (HPI). For health risk assessment (HRA), chronic daily intake (CDI) and hazard quotient (HQ) were calculated using USEPA methods. ArcGIS v10.3 software was applied to plot spatial maps for various parameters using the inverse distance weighted (IDW) interpolation method.

Heavy metal pollution index

Heavy metal pollution index (HPI) was applied to assess the overall impact of individual metals on groundwater quality. HPI is computed using the rating and weight of each metal. The rate is an arbitrary value between 0 and 1, and weight

is inversely proportional to the international drinking water standards of individual metals (Mohan et al. 1996; Edet and Offiong 2002; Rajmohan et al. 2022). HPI is computed by the following Eq. (1)

$$\text{HPI} = \frac{\sum_{i=1}^n W_i Q_i}{\sum_{i=1}^n W_i} \quad (1)$$

where Q_i is sub-index of i th metal, W_i is the unit weight of the i th metal, and n is the number of metals considered.

The sub-index (Q_i) is computed using Eq. (2)

$$Q_i = \sum_{i=1}^n \frac{M_i - L_i}{S_i - L_i} \times 100 \quad (2)$$

where M_i is the measured concentration of the metal in the i th sample and L_i and S_i are the lower desirable limit (LDL) and maximum permissible limit (MPL) of i th metal, respectively. For LDL and MPL, WHO (2017) and USEPA (2012) recommended drinking water standards were used (Table 1).

Contamination index

The contamination index (C_d) is widely employed to appraise metal pollution in drinking water and several studies applied this index worldwide (Mohan et al. 1996; Backman et al. 1998; Basahi et al. 2018). This index is more appropriate to compute the cumulative impact of pollutants (trace metals) in the groundwater. C_d is calculated using Eqs. (3) and (4).

$$C_d = \sum_{i=1}^n C_{f_i} \quad (3)$$

Table 1 LDL, MPL, W_i and RfD used in the HPI, C_d and HRA calculations

Metals	LDL (µg/l)	MPL (µg/l)	Weightage (W_i)	RfD (mg/kg/day)
Ag	0	100	0.0100	0.005
Al	50	200	0.0050	0.0004
B	0	500	0.0020	0.2
Ba	700	2000	0.0005	0.2
Cr	50	100	0.0100	0.003
Cu	1300	2000	0.0005	0.005
Fe	300	1000	0.0010	0.7
Li	0	10	0.1	0.002
Mn	50	400	0.0025	0.14
Mo	0	70	0.0143	0.005
Ni	0	20	0.0500	0.02
Pb	10	15	0.0667	0.0036
Sr	0	4000	0.00025	0.6
V	0	20	0.0500	0.009
Zn	3000	5000	0.0002	0.3

$$Cf_i = \frac{C_{Mi}}{C_{Li}} - 1 \tag{4}$$

where Cf_i is the contamination factor, C_{Mi} and C_{Li} are measured concentration and the maximum permissible limit (MPL) of the i th metal recommended by the WHO (2017), respectively.

Multivariate statistical analysis

Multivariate statistical analysis (MSA) including Pearson correlation analysis, principal component analysis (PCA) and Hierarchical cluster analysis (HCA) was adopted using SPSS v16.0. To eliminate the bias in the analysis, data were log-transformed and standardized. Further, standard scores (z-score) were used to get a dimensionless data set, which eliminates the variables unit’s impact (Güler et al. 2002; Barzegar et al. 2019; Ren et al. 2021). In both PCA and HCA, 17 variables (EC, pH, Ag, Al, B, Ba, Cr, Cu, Fe, Li, Mn, Mo, Ni, Pb, Sr, V, and Zn) were employed. Sample numbers 1, 5 and 11 are excluded from the MSA analysis due to extreme salinity and metals. In the PCA, the varimax rotation method with Kaiser normalization was adopted (Kaiser 1960). A principal component with an eigenvalue greater than one was extracted for interpretation. HCA was carried out using the Ward method with the squared Euclidean distance (Ward 1963).

Health risk assessment

Health risk for adults and children due to trace metals pollution is often caused by the oral injection of polluted drinking water. Other pathways such as dermal contacts and inhalation are insignificant compared to oral consumption. In this study, USEPA-recommended methods are adopted to compute the chronic daily intake (CDI, mg/kg/day) and hazard quotient (HQ) (USEPA 2011). The CDI for each trace metal is calculated by Eq. (5).

$$CDI_{oral} = \frac{C \times IR \times EF \times ED}{BW \times AT} \tag{5}$$

where C represents the measured concentration of metal in the groundwater (mg/l) and IR is ingestion rate (l/day) (adults 2.5; children 0.78) (USEPA 2014). EF (days/year) and ED (years) are exposure frequency (365 days) and exposure duration (adults 70 and children 6), respectively (Nar-simha and Rajitha 2018; Kadam et al. 2019). Likewise, BW represents average body weight (kg) (adults 65 and children 15). AT (average exposure time, days) is calculated by the multiplication of ED and EF .

The non-carcinogenic risk of each metal is estimated using the hazard quotient (HQ_{oral}) using Eq. (6) (USEPA 1989).

$$HQ_{oral} = \frac{CDI_{oral}}{RfD} \tag{6}$$

where RfD represents the oral reference dose (mg/kg/day) of each trace metal, which is provided in Table 1 (USEPA 1993, 2019). Finally, the hazard index (HI) for each groundwater sample is estimated by the summation of HQ_{oral} values of each metal using the Eq. (7)

$$HI = \sum_{i=1}^n HQ_i \tag{7}$$

Groundwater samples with $HI < 1$, $CDI_{oral} < 1$ and $HQ_{oral} < 1$ are suitable for drinking without any health hazards whereas higher values (> 1) produce potential non-carcinogenic health risks to the consumer.

Results and discussion

Table 2 illustrates the descriptive statistics calculated for pH, EC, TDS and trace metals analysed in this study. In this aquifer, groundwater is slightly acidic to alkaline and pH ranged from 6.6 to 7.8 with an average of 7.3. The electrical conductivity (EC) varied from 782 to 22,500 μ S/cm with a mean value of 4292 μ S/cm. Similarly, total dissolved solids (TDS) calculated from EC ($TDS = EC \times 0.64$) ranged from 391 to 11,240 mg/l with an average of 2145 mg/l. The standard deviation of both EC and TDS is 4645 μ S/cm and 2321 mg/l, respectively, which implies that groundwater

Table 2 Descriptive statistics for pH, EC, TDS and metals analysed

$N=59$	Unit	Min	Max	Average	STD
pH		6.6	7.8	7.3	0.2
EC	μ S/cm	782	22,500	4292	4645
TDS	mg/l	391	11,240	2145	2321
Ag	μ g/l	BDL	640	54	127
Al	μ g/l	19	479	100	110
B	μ g/l	184	10,300	1378	1618
Ba	μ g/l	12	387	93	70
Cr	μ g/l	17	501	101	108
Cu	μ g/l	BDL	2440	276	467
Fe	μ g/l	74	1020	254	229
Li	μ g/l	19	432	99	102
Mn	μ g/l	17	897	72	123
Mo	μ g/l	15	2280	255	355
Ni	μ g/l	17	623	122	134
Pb	μ g/l	6	196	39	44
Sr	μ g/l	422	34,339	5513	6497
V	μ g/l	BDL	469	36	80
Zn	μ g/l	19	335	79	76

chemistry is governed by various processes and sources. The spatial distribution map of EC illustrates that there is no trend in the EC (Supplementary Figure SF1). Few wells in the northeast and southern regions have higher values. Most of the areas in the central region have low values ($EC < 3000 \mu\text{S}/\text{cm}$ and $< 5000 \mu\text{S}/\text{cm}$). In contrast to this observation, extreme values are recorded in the downstream coastal region.

Trace metals distribution and drinking water quality assessment

Descriptive statistics of trace metals analysed in this study are provided in Table 2. Similarly, spatial distribution maps of trace metals are presented as supplementary Figures SF1 to SF3. The trace metal concentrations analysed in the groundwater were compared with WHO guideline (GV) values and the United States Environmental Protection Agency (USEPA) maximum contamination level (MCL) recommended for drinking water (Table 3) (USEPA 2012; WHO 2017). The concentration of Ag ranged from below the detection limit (BDL) to $640 \mu\text{g}/\text{l}$ (average $54 \mu\text{g}/\text{l}$) and 15% of samples exceeded the WHO standard limits ($100 \mu\text{g}/\text{l}$), which are unfit for consumption (Tables 2, 3, Fig. 2a). The spatial distribution of Ag depicts that it is less than $50 \mu\text{g}/\text{l}$ in almost 80% of the study area and higher values were noticed in a few wells in northern and southern regions (Figure SF3). The groundwater Al concentration varied from 19 to $479 \mu\text{g}/\text{l}$ with a mean of $100 \mu\text{g}/\text{l}$ and 15% of samples surpassed the GV ($200 \mu\text{g}/\text{l}$) whereas 46% of samples exceeded

the MCL values ($50 \mu\text{g}/\text{l}$) (Tables 2, 3, Fig. 2a), which are not recommended for drinking application. High Al in drinking water causes various health issues for the consumer such as arthritic pain, and vomiting, and affects the nervous system (WHO 2003c). Like Ag, the concentration of Al in the central part of the study area is also low (< 50) and higher values have appeared in the north-eastern, southern and western regions (Figure SF2). Al-Hobaib et al., (2013) and Basahi et al. (2018) also documented high Al concentrations in groundwater in Saudi Arabia.

The concentration of B is between 184 and $10,300 \mu\text{g}/\text{l}$ (average $1378 \mu\text{g}/\text{l}$) (Table 2). Table 3 and Fig. 2a depict that 78% of samples exceeded the WHO recommended guideline values and are not advisable for drinking. Basahi et al. (2018) also reported high B content in groundwater in Jazan province, Saudi Arabia. Like Al, high B also creates health problems for consumers, namely vomiting, abdominal pain and diarrhoea (WHO 2003a). The spatial distribution pattern of B shows a similar trend to EC and the central region expresses lower values and extreme values recorded in the coastal region. Further, higher values ($> 2000 \mu\text{g}/\text{l}$) also appeared in the northern region (Well numbers 40, 42). Groundwater Ba concentration is from 12 to $387 \mu\text{g}/\text{l}$ (mean $93 \mu\text{g}/\text{l}$), and it is within the recommended limit for drinking (Tables 2, 3, Fig. 2a). The spatial distribution map indicates a different trend, and high concentrations are noticed in the central region (Figure SF3).

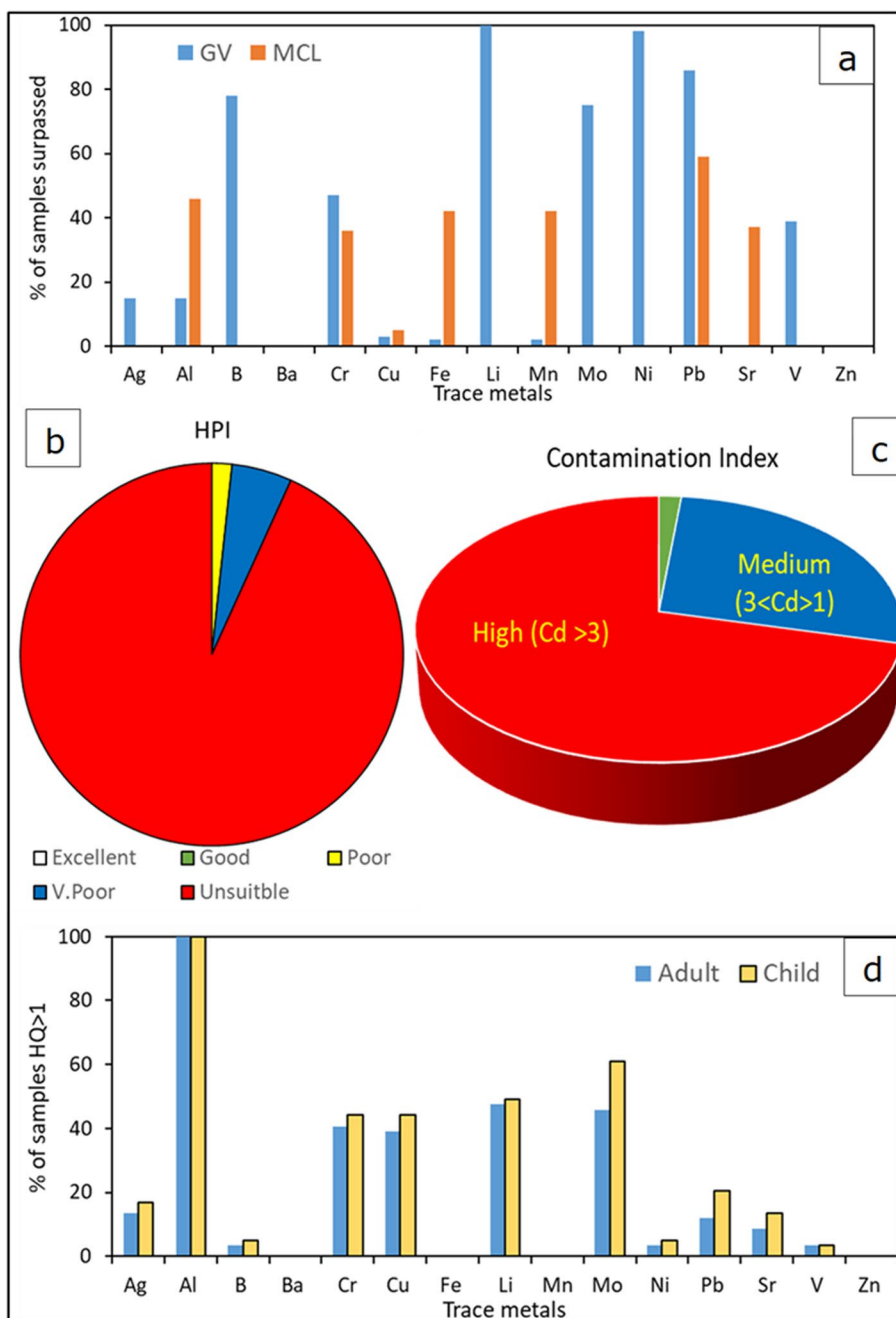
The range of Cr concentration in the groundwater is from 17 to $501 \mu\text{g}/\text{l}$ (average $101 \mu\text{g}/\text{l}$) (Table 2). Table 3 and Fig. 2a denote that 47 and 36% of samples surpassed the GV and MCL, respectively, and were unfit for drinking at the study site. Haemorrhagic diathesis, gastrointestinal disorders and lung cancer are common health issues resulting from high Cr drinking water (WHO 2003d). Figure SF2 illustrates that downstream wells and a few wells that existed in northern and southern regions express high concentrations in the study site. But the occurrence of Cr in the central region is low ($< 50 \mu\text{g}/\text{l}$). The concentration of Cu varied from BDL to $2440 \mu\text{g}/\text{l}$ with an average of $276 \mu\text{g}/\text{l}$ (Table 2). In most of the samples, the concentration is within the recommended limit (Table 3, Fig. 2a). The Cu concentration is generally less than $500 \mu\text{g}/\text{l}$ and uniformly distributed in the study area except for a few locations in the downstream region (Figure SF1).

In the study area, Fe concentration is between 74 and 1020 (mean $254 \mu\text{g}/\text{l}$) and the Fe concentration in 98% of samples is within the drinking water limit recommended by WHO ($1000 \mu\text{g}/\text{l}$); however, 42% of samples exceeded the MCL ($300 \mu\text{g}/\text{l}$) recommended by USEPA (Tables 2, 3, Fig. 2a). Figure SF2 illustrates that Fe concentration is less than $300 \mu\text{g}/\text{l}$ in most of the sites and high values are noticed in the downstream wells and a few wells in the northern and southern regions. The concentration of Li is from 19

Table 3 Metals contamination status in groundwater and water usability assessment using WHO and USEPA standards

Metals	Drinking water limit ($\mu\text{g}/\text{l}$)		Samples surpassed (%)	
	WHO GV	USEPA MCL	GV	MCL
Ag	100	–	15	–
Al	200	50	15	46
B	500	–	78	–
Ba	700	2000	–	–
Cr	50	100	47	36
Cu	2000	1300	3	5
Fe	1000	300	2	42
Li	10	–	100	–
Mn	400	50	2	42
Mo	70	–	75	–
Ni	20	–	98	–
Pb	10	15	86	59
Sr	–	4000	–	37
V	20	–	39	–
Zn	3000	5000	–	–

Fig. 2 Water samples surpassed the guideline value (GV) and maximum contamination level (MCL) (a), water pollution status (b, c) and health risk assessment (HRA) results (d) in the Wadi Fatimah basin



to 432 µg/l with an average of 99 µg/l and all the samples exceeded the drinking water recommended limit (Tables 2, 3, Fig. 2a). Li also behaves like Fe and the central region has low values, whereas enrichment is observed in a few wells in the northern, southern and western regions.

Groundwater Mn concentration ranged from 17 to 897 µg/l (mean 72 µg/l) and almost 98% of samples are within the drinking water limit recommended by WHO (Tables 2, 3, Fig. 2a). However, 42% of samples surpassed MCL and are not advisable for consumption. Figure SF1 indicates that Mn concentration in the central part of the

study site is less than 50 µg/l and in most of the area, it is less than 200 µg/l. The concentration of Mo varied from 15 to 2280 µg/l (average 255 µg/l) and 75% of samples surpassed the WHO GV (70 µg/l) that are unsuitable for drinking application (Tables 2, 3, Fig. 2a). The spatial distribution of Mo illustrates that in most of the region, the concentration is between 70 and 300 µg/l and the elevated concentrations are recorded in the downstream wells (Figure SF1).

The concentration range of Ni and Pb is 17–623 µg/l and 6–196 µg/l with an average of 122 and 39 µg/l, respectively (Table 2). In the case of Ni, 98% of samples are

not recommended for drinking which exceeded the drinking water limit (20 µg/l) (Table 3, Fig. 2a). In the case of Pb, 86% and 59% of samples surpassed the GV and MCL, respectively and are unfit for drinking usage (Table 3, Fig. 2a). Drinking water with high Ni and Pb results in various health problems, namely neurological disorders, lung cancer, gastrointestinal distress, reduced lung function and chronic bronchitis (WHO 2003b). Figure SF2 expresses that the spatial distribution trend of both Ni and Pb are similar and groundwater in the central region has low values and enrichment is observed in three zones (north, south and west) like other metals.

The concentration of Sr ranged from 422 to 34,339 µg/l (mean 5513 µg/l) and 37% of samples surpassed the MCL which is not appropriate consumption (Tables 2, 3, Fig. 2a). Like other metals, the central region has lower concentrations and high concentrations are noticed in some pockets in the northern region as well as downstream regions. However, wells with high concentrations in downstream are located far from the coast. Likewise, the concentration of V also expresses a different trend compared to other metals and the lowest concentrations (<20 µg/l) are noticed in the high salinity wells that existed in the northern and southern regions (Figure SF3). High values appeared in some pockets in the central region and downstream. In this study, V concentration ranged from BDL to 469 µg/l with an average of 36 µg/l (Table 2). Table 3 and Fig. 2a describe that 39% of samples are not suitable for drinking and surpassed the WHO recommended GV. Asthma, lung cancer, rhinitis and respiratory problems are common health complications to the consumer owing to high V drinking water (WHO 2001; ATSDR 2020). The concentration of Zn in the groundwater is between 19 and 335 µg/l with a mean of 79 µg/l (Table 2). According to USEPA and WHO drinking water standards, Zn concentration is within the recommended limit in this aquifer. Like other metals, high concentrations occurred in the few wells in northern, southern and western regions (Figure SF2). The Zn concentration is generally <100 µg/l in most of the study areas.

Figure 2a illustrates the pictorial representation of metal pollution status at the study site. It illustrates that extreme pollution, based on the percentage of samples surpassed, is observed by the Li followed by the Ni > Pb > B > Mo > Cr > Al > Fe = Mn > V > Sr > Ag > Cu. The concentrations of Ba and Zn in this aquifer are within the drinking water recommended limit.

Integrated trace metals pollution assessment

Heavy metals pollution index

The heavy metals pollution index (HPI) was computed using Eqs. (1) and (2) and its descriptive statistics are stated in

Table 4. Table 4 indicates that HPI ranged from 56 to 2848 with an average of 592. Groundwater samples were classified into five classes using HPI values, namely excellent (0–25), good (26–50), poor (51–75), very poor (75–100) and unsuitable (> 100) (Basahi et al. 2018). Figure 2b poses the pictorial representation of this classification in the study area. Almost 93% of samples are not appropriate for drinking due to high metal load. The remaining 7% of samples fall into poor (2%) and very poor (5%) classes. Overall, the groundwater in this basin is not recommended for drinking and requires proper treatment before distribution.

Contamination index

Like HPI, the contamination index (C_d) is also an important parameter to appraise the pollution status in any aquifer. In this study, it is calculated using Eqs. (3) and (4) and the descriptive statistics are rendered in Table 4. The C_d value in the groundwater ranged from 1 to 155 with a mean of 23. Like HPI, water contamination status is assessed using C_d and classified into three classes such as low ($C_d < 1$), medium ($1 > C_d < 3$) and high ($C_d > 3$) contamination. In the study site, well number 27 only comes under the low contamination class. According to the C_d classification, 27% of samples fall medium contamination category, while 71% of samples are belongs to the high contamination class (Fig. 2c).

Figure 3 depicts that groundwater with medium contamination is observed in the central part of the study area. In the remaining area, the groundwater is highly polluted by metals. Figures SF1-SF3 also well resembled this observation because the low concentrations of most of the metals are recorded in the central part of the study area. Depth to groundwater level also shows that deep water levels are recorded in the central part of the study site (Fig. 1b).

Appraisal of pollution sources using multivariate statistical analysis

Pearson correlation matrix

Pearson correlation matrix is employed to explore the inter-relationship between the variables and to identify their sources in groundwater (Table 5). Table 5 shows the results,

Table 4 Descriptive statistics for HPI, Cd and HI computed

	Minimum	Maximum	Average	STD
HPI	56	2848	592	649
C_d	1	155	23	30
HI Adults	3.0	105	18.8	21.4
HI Children	4.0	142	25.4	28.9

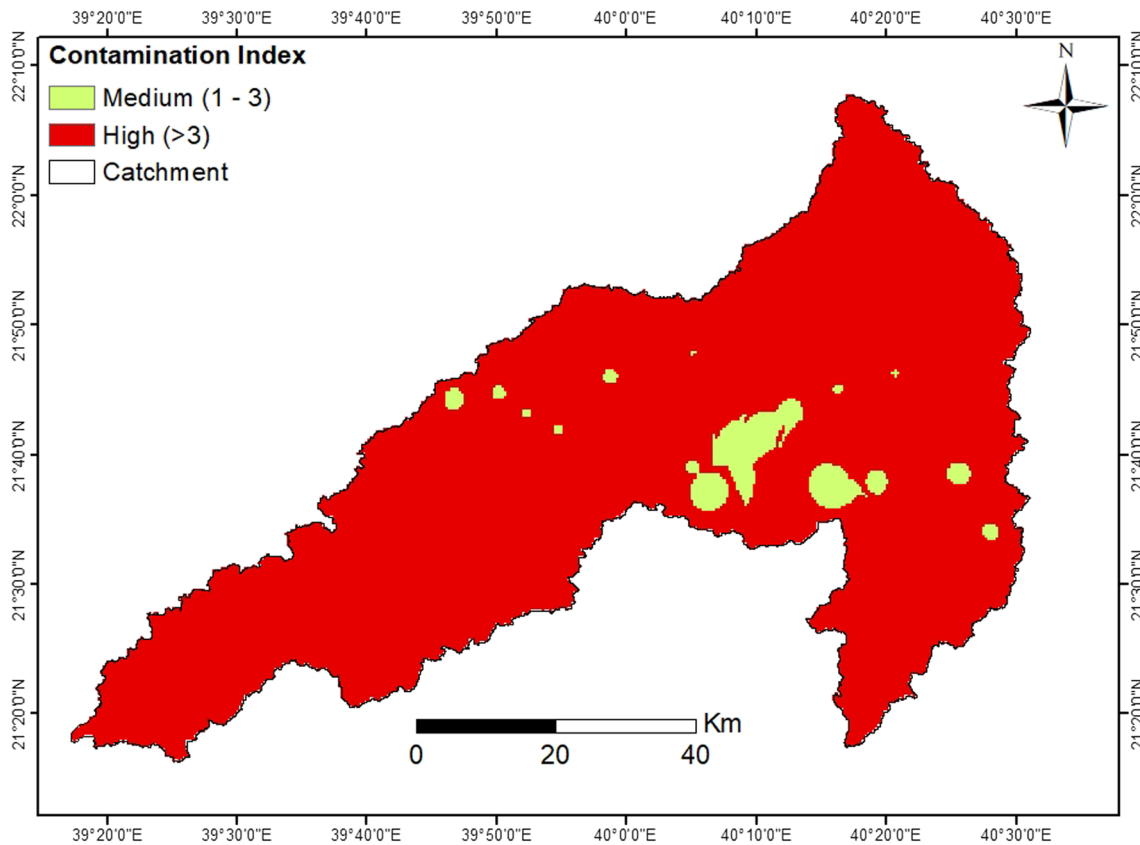


Fig. 3 Spatial distribution of contamination index in the Wadi Fatimah basin

Table 5 Results of Pearson correlation analysis

	EC	pH	Ag	Al	B	Ba	Cr	Cu	Fe	Li	Mn	Mo	Ni	Pb	Sr	V	Zn
EC	1.00																
pH	-0.56	1.00															
Ag	0.12	-0.26	1.00														
Al	0.93	-0.58	0.38	1.00													
B	0.84	-0.40	0.05	0.74	1.00												
Ba	0.24	-0.42	0.10	0.32	-0.01	1.00											
Cr	0.83	-0.54	0.54	0.96	0.70	0.23	1.00										
Cu	0.84	-0.41	0.35	0.83	0.85	0.00	0.81	1.00									
Fe	0.84	-0.52	0.36	0.90	0.75	0.19	0.92	0.73	1.00								
Li	0.55	-0.46	0.70	0.67	0.48	0.14	0.74	0.58	0.80	1.00							
Mn	0.87	-0.53	0.32	0.92	0.75	0.23	0.91	0.73	0.99	0.77	1.00						
Mo	0.80	-0.46	0.12	0.78	0.73	0.26	0.73	0.70	0.72	0.46	0.74	1.00					
Ni	0.83	-0.55	0.55	0.96	0.68	0.25	0.99	0.81	0.89	0.71	0.89	0.74	1.00				
Pb	0.83	-0.56	0.58	0.96	0.67	0.27	0.99	0.82	0.87	0.74	0.87	0.72	0.99	1.00			
Sr	0.94	-0.59	0.13	0.91	0.73	0.32	0.81	0.77	0.78	0.49	0.81	0.78	0.82	0.83	1.00		
V	0.09	-0.11	-0.12	0.03	0.11	0.16	0.01	0.07	-0.02	-0.09	-0.01	0.53	0.02	0.01	0.11	1.00	
Zn	0.86	-0.56	0.49	0.95	0.73	0.24	0.97	0.80	0.98	0.81	0.97	0.74	0.96	0.96	0.81	-0.01	1.00

Bold values indicate significant correlation and highly loaded variables, respectively

and the correlation coefficient values greater than 0.6 are considered for further discussion. Variables, namely pH, Ba and V, are not correlating with other variables. Likewise, variables such as Ag, Ba and V are not correlating with Al, Fe, EC, B and Sr. Li also behaves like Ag and is not correlating with EC, B and Sr. Al has a significant ($p < 0.01$) strong positive correlation with Cr ($r = 0.96$), Ni ($r = 0.96$), Pb ($r = 0.96$), Zn ($r = 0.95$), EC ($r = 0.93$), Mn ($r = 0.92$), Sr ($r = 0.91$), Fe ($r = 0.90$), Cu ($r = 0.83$) and significant ($p < 0.01$) positive correlation with Mo ($r = 0.78$), B ($r = 0.74$) and Li ($r = 0.67$). Similarly, Fe has a strong positive correlation with Mn ($r = 0.99$), Zn ($r = 0.98$), Cr ($r = 0.92$), Al ($r = 0.90$), Ni ($r = 0.89$), Pb ($r = 0.87$), EC ($r = 0.84$), Li ($r = 0.80$), Sr ($r = 0.78$), B ($r = 0.75$), Cu ($r = 0.73$) and Mo ($r = 0.72$). Mn is correlated well with Fe ($r = 0.99$), Zn ($r = 0.97$), Al ($r = 0.92$), Cr ($r = 0.91$), Ni ($r = 0.89$), Pb ($r = 0.87$), EC ($r = 0.87$), Sr ($r = 0.81$), Li ($r = 0.77$), B ($r = 0.75$), Mo ($r = 0.74$) and Cu ($r = 0.73$). In this study, Fe, Mn and Al express a strong positive correlation with each other. Further, metals originating from geogenic sources generally expose a strong positive correlation with Fe, Mn and Al (GAE 2005; Badr et al. 2009; Rajmohan et al. 2020, 2022). As an aforementioned, volcanic formation, mafic rocks and basaltic rocks are the predominant rock types in the study site and these geological formations have enormous metals in various forms, namely oxides, hydroxides, carbonates and sulphides, and are associated with silicates (Alyamani and Hussein 1995; Reimann et al. 2003; Salminen et al. 2005; Ahmed et al. 2017; Rajmohan et al. 2022). Weathering and dissolution of these formations mostly likely accumulate the trace metals in this aquifer.

Principle component analysis

Principle components analysis (PCA) was adopted to appraise the source of trace metals in this aquifer. In this study, PCA resulted in three PCs with eigenvalue > 1 (Table 6), which explains 85% of the total variance (Table 6). The PCs scores were plotted to demark the influence of each PC in the study area (Fig. 4).

PC1 is the most significant and explains 57% of the total variance. The variables, namely EC, B, Al, Sr, Cu, Mn, Fe, Zn, Cr, Mo, Ni and Pb, are highly loaded in the PC1. High loading of Al, Mn and Fe suggests that the weathering of aluminium silicates and oxides/hydroxides of Fe and Mn are predominant sources of these metals in the study site (Badr et al. 2009; Rajmohan et al. 2014, 2017). Moreover, the concentration of Cu (3 $\mu\text{g/l}$), Mn (2 $\mu\text{g/l}$), Zn (10 $\mu\text{g/l}$), Cr ($< 0.05 \mu\text{g/l}$), Mo (10 $\mu\text{g/l}$), Ni (7 $\mu\text{g/l}$) and Pb (0.3 $\mu\text{g/l}$) in the seawater is very low (Hem 1985). Further, groundwater head varies from 13 to 1924 m above MSL, which rules out the possibilities for saline water invasion and marine origin of these metals in the study area. Thus, enrichment of

Table 6 Results of principal component analysis

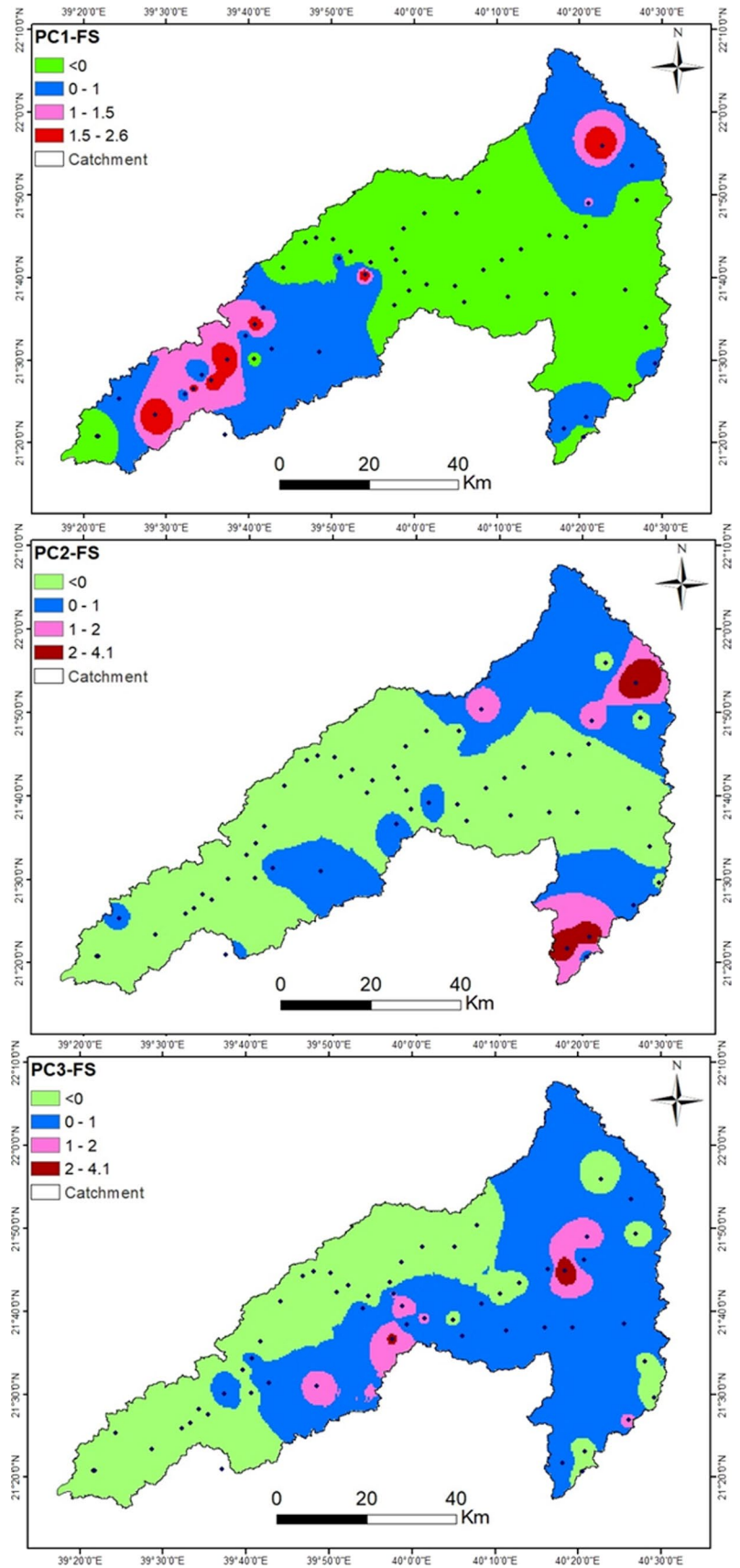
Variables	Principle components		
	PC1	PC2	PC3
pH	-0.44	-0.24	-0.56
EC	0.95	0.04	0.18
Ag	0.13	0.87	0.12
Al	0.90	0.30	0.25
B	0.92	-0.09	-0.08
Ba	0.02	0.13	0.86
Cr	0.85	0.45	0.19
Cu	0.89	0.15	-0.04
Fe	0.87	0.36	0.12
Li	0.56	0.68	0.10
Mn	0.88	0.33	0.15
Mo	0.84	-0.14	0.39
Ni	0.84	0.44	0.22
Pb	0.82	0.47	0.23
Sr	0.88	0.05	0.29
V	0.13	-0.51	0.53
Zn	0.87	0.44	0.18
Total	9.7	2.8	1.9
% of Variance	57	17	11
Cumulative %	57	73	85

Bold values indicate significant correlation and highly loaded variables, respectively

these metals (Al, Cr, Cu, Fe, Mo, Ni, Pb, Zn) in the downstream wells is caused via weathering of respective minerals followed by evaporation (Figure SF1-SF3) (Salminen et al. 2005). The elevated concentration of Cr and Ni in ultramafic rocks is reported (Salminen et al. 2005). Likewise, Pb is mostly associated with clay minerals, organic matter, Al/Fe hydroxides and Mn oxides, which influence the Pb concentration in groundwater. Alyamani and Hussein (1995) reported various rock types and minerals in this basin, namely granodiorite (hornblende, biotite, oligoclase), chlorite schist (epidote, chlorite), metabasalt (actinolite, albite, chlorite), diorite (andesine, hornblende, biotite) and granite. Further, flash flood and groundwater flow from upstream to downstream seem to be accumulated these metals in the downstream wells (Basahi et al. 2018).

However, high loading of EC, B and Sr reveals that apart from weathering, other sources such as evaporation, dissolution of evaporites and infiltration of highly evaporated irrigation water from the agricultural field are likely contributing to the groundwater quality (Esmaeili et al. 2018). Spatial distribution of B and EC shows that elevated concentrations occurred in the coastal region as well as two wells in the north-eastern region (Figure SF1). Ure and Berrow (1982) reported the accumulation of hydrated borate minerals in the evaporite deposits in an arid environment. Hence, the dissolution of evaporites

Fig. 4 Spatial variation of principal components PC1, PC2 and PC3 in the Wadi Fatimah basin



is likely governed by both EC and B in the downstream wells. Likewise, the enrichment of these variables in the upstream region suggests the impact of long storage of groundwater, which facilitates the rock-water interaction. The spatial distribution pattern of Sr illustrates that high concentrations are noticed in the wells located far from the coast in downstream as well as a few wells in the northern region (Figure SF1). Further, Sr is a lithophilic element and belongs to group 2 in the periodic table. Hence, it can easily substitute with carbonates, sulphates, gypsum, plagioclase and other silicates (Mielke 1979). Dissolution of these minerals enhances the Sr concentration in this aquifer along with evaporation.

The spatial distribution of the PC1 score (Fig. 4) explains that the highest values appeared in the downstream region (well numbers 10, 18) as well as in two wells (well numbers 42, 40) in the northern region. Overall, PC1 explains that the predominant source of these metals is mineral weathering, evaporation, and irrigation return flow followed by evaporite dissolution in the groundwater (Barzegar et al. 2019).

The PC2 represents 17% of the total variance and is associated with Ag and Li. Further, moderate negative loading of V is noticed in this PC. The spatial distribution of Ag depicts that high concentrations occurred in the northern and southern regions. In the rest of the area, the Ag concentration is less than 50 µg/l (Figure SF3). Hence, rock–water interaction is the primary source of this metal in the study area (GAE 2005; Al-Shanti 2009). Similarly, the spatial distribution of Li shows that wells in downstream, northern and southern regions have high concentrations. The Li concentration in the seawater is 170 µg/l. In the study site, the Li concentration in 15% of samples exceeded the seawater concentration and the maximum concentration is 432 µg/l, which ruled out the marine origin and reveals the impact of evaporation. The primary source for

Li is silicate minerals and Li occurs as an accessory element in feldspar, amphibole and biotite mica (GAE 2005; Panda et al. 2020). Hence, Li is derived from the geogenic origin followed by evaporation. Figure 4 depicts the highest positive score of PC2 in the northern and southern regions where groundwater is largely regulated by the weathering processes facilitated by the long storage and evaporation.

PC3 explains only 11% of the total variance and Ba and V are loaded positively, whereas pH is loaded negatively. As aforementioned, both Ba and V are not correlating with other metals (Table 6). The spatial distribution pattern expresses that both are enriched in the central part of the study area (Figure SF3). In addition, V shows enrichment in the downstream wells. Ba is mostly derived from weathering of mafic rocks and basalt in the study site (Mielke 1979; Ure and Berrow 1982). However, Ba is not correlating with Fe and Al in this study. Hence, the dissolution of carbonate (Witherite (BaCO₃)) and sulphate minerals (Barite (BaSO₄)) is most likely the primary control of Ba concentration in the groundwater (Massey and Barnhisel 1972; Aiuppa et al. 2000). Barite is one of the important minerals in evaporite (Senior and Sloto 2006). In the case of V, basaltic and mafic rocks and volcanic emissions are predominant geogenic sources for this metal (Mielke 1979; Taylor et al. 1979). The spatial distribution of this PC indicates that the highest positive scores are identified in well number 38 followed by 31 and 29 and the groundwater chemistry in the central part of the study area is governed by the mineral weathering processes.

Hierarchical cluster analysis (HCA)

Hierarchical cluster analysis (HCA) was also performed to investigate the potential sources of trace metals in the study

Fig. 5 Dendrogram resulted from R-mode (variables) HCA analysis

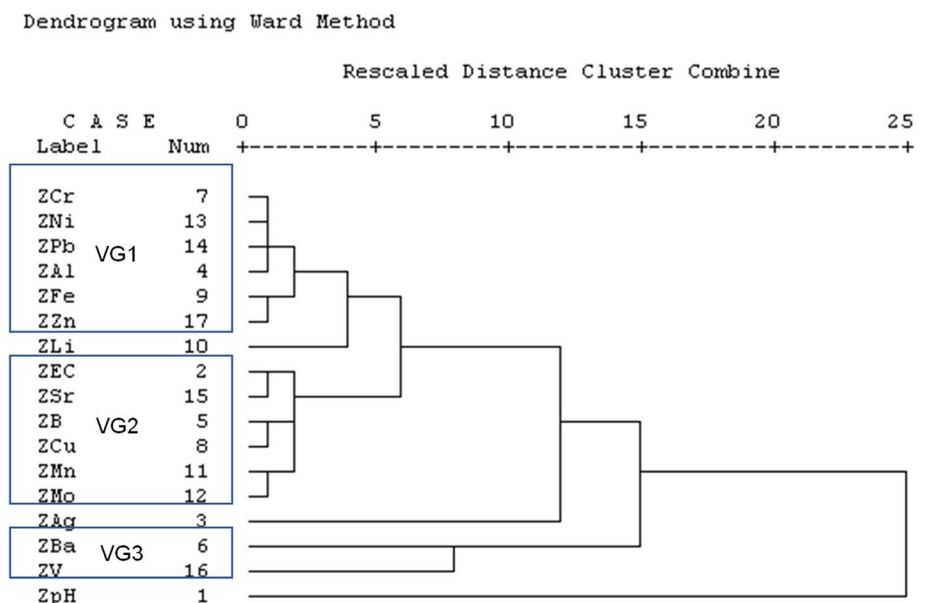
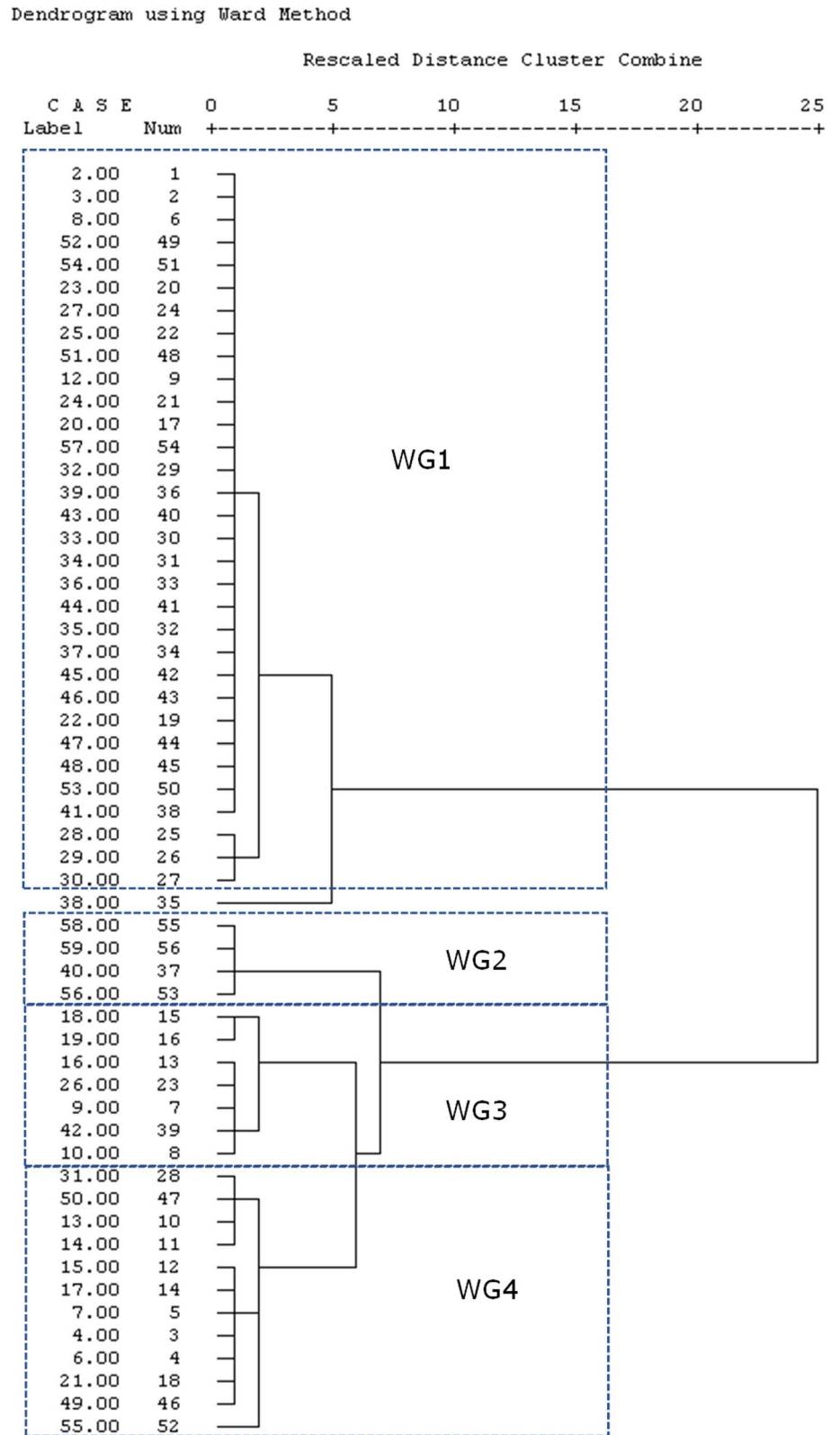


Fig. 6 Dendrogram resulted from Q-mode (wells) HCA analysis



site. In this study, R-mode (variables) and Q-mode (wells) HCA were performed (Figs. 5, 6). R-mode HCA resulted in three major clusters as VG1, VG2 and VG3 and VG1

shows the association of Cr, Ni, Pb, Al, Fe, and Zn. Loading of Al, Fe and Mn in this cluster strongly suggests the role of mineral dissolution (aluminium silicates, Fe/Mn oxides/

hydroxides) on water chemistry (Badr et al. 2009; Arslan et al. 2017; Rajmohan et al. 2017, 2022). The association of EC, Sr, B, Cu, Mn and Mo in VG2 indicates the influences of irrigation return flow, evaporation, evaporite dissolution and mineral weathering (Abiye and Leshomo 2014; Lima et al. 2014; Barzegar et al. 2019; Al-Bagawi et al. 2021; Rajmohan et al. 2022). In the PCA, variables loaded in PC1 are clustered in VG1 and VG2. The Ba and V are associated with VG3 and both are highly loaded in PC3 and accumulated in the groundwater through geogenic processes. Further, Li, Ag and pH are not associated with any variables in this classification, which are highly loaded in PC2.

Q-mode cluster analysis clustered the wells with similar chemical characteristics. In this study, Q-mode HCA resulted in 4 clusters as WG1, WG2, WG3 and WG4 and well number 38 is not associated with any cluster (Fig. 6). The descriptive statistics of each cluster are presented in Table 7. The average concentration of each variable in each cluster is plotted in Fig. 7a. Based on the average of EC, the clusters follow the following decreasing order: WG3 > WG2 > WG4 > WG1. However, the average concentrations of variables indicate that samples in WG3 and WG2 are extremely polluted compared to other clusters.

Table 7 and Fig. 7a depict that variable concentrations are generally low in cluster WG1 and the average pH is slightly higher than in other clusters. Further, 58% of samples are associated with WG1 and EC varied from 782 $\mu\text{S/cm}$

cm to 2840 $\mu\text{S/cm}$ (Average, 1716 $\mu\text{S/cm}$) (Table 7). Wells clustered in WG1 are mostly located in the upstream and central parts of the study area (Fig. 7b). In the central region, groundwater metal concentrations are generally low (Figures SF1–SF3) and the water chemistry is predominantly governed by the geogenic sources.

In the WG4, the average concentrations of trace metals are higher than the WG1 but lower than WG2 and WG3 (Fig. 7a, Table 7). The mean of Ag, Ba and Li in WG4 is greater than that in WG3. Further, 22% of samples are clustered in this cluster and EC ranged from 1403 $\mu\text{S/cm}$ to 6520 $\mu\text{S/cm}$ with a mean of 4190 $\mu\text{S/cm}$. The spatial distribution pattern illustrates that these wells are located in the downstream (western region) region and far from the coast (Fig. 7b). Table 7 exhibits that 80% of samples are belongs to WG1 (58%) and WG4 (22%) clusters in the study area.

Four samples (7%) are associated with cluster WG2 and EC is between 3790 $\mu\text{S/cm}$ and 6150 $\mu\text{S/cm}$ (average 4875 $\mu\text{S/cm}$). In this cluster, the average concentration of Ag, Ba, Cr, Fe, Ni, Pb, Zn and Li are higher than in other clusters; however, the concentration of V is below the detection limit. Figure 7 demonstrates that these wells have existed in the northern and southern regions (upstream). High EC values in the upstream wells imply that the water chemistry is predominantly affected by rock–water interaction triggered by the long storage and evaporation.

Table 7 Descriptive statistics of various variables for HCA groups

WG1 (N=32)																	
	pH	EC	Ag	Al	B	Ba	Cr	Cu	Fe	Ni	Pb	Zn	Mo	V	Li	Mn	Sr
Min	7.1	782	BDL	19	184	12	17	1	74	17	6	19	15	BDL	19	17	422
Max	7.8	2840	173	90	1510	204	102	195	130	136	42	53	188	151	53	31	3784
Average	7.4	1716	12	35	592	74	32	61	85	41	13	27	80	17	27	20	1964
STD	0	535	36	13	297	46	15	52	10	21	6	6	36	27	9	3	871
WG2 (N=4)																	
Min	6.94	3790	317	142	925	74	209	320	436	246	76	145	204	BDL	163	96	3095
Max	7.32	6150	640	228	2075	168	272	605	486	345	106	172	408	BDL	399	112	14,020
Average	7.11	4875	443	182	1406	105	236	423	462	288	93	162	291	–	248	102	7113
STD	0.16	1143	139	40	484	43	28	132	21	44	12	12	100	–	104	7	4796
WG3 (N=7)																	
Min	6.85	6320	BDL	110	2120	42	112	471	380	125	38	103	245	BDL	124	87	6520
Max	7.51	11,580	98	246	4630	122	277	825	510	352	110	177	635	101	164	122	18,270
Average	7.13	9107	18	198	3008	75	191	664	450	235	76	142	483	46	138	106	12,762
STD	0.22	2140	36	49	843	28	52	111	41	71	23	24	138	38	13	13	4055
WG4 (N=12)																	
Min	6.85	1403	BDL	44	426	37	53	1	111	56	16	47	50	BDL	116	22	715
Max	7.67	6520	289	185	1870	218	177	411	450	215	68	148	392	68	265	105	8720
Average	7.23	4190	31	101	1318	94	108	163	362	119	37	98	231	19	153	83	5119
STD	0.20	1294	83	44	370	63	39	169	85	50	15	26	98	25	43	21	2955

Sample numbers 1, 5 and 11 are excluded in the MSA. Sample number 38 is not associated with any cluster and is not included in the table

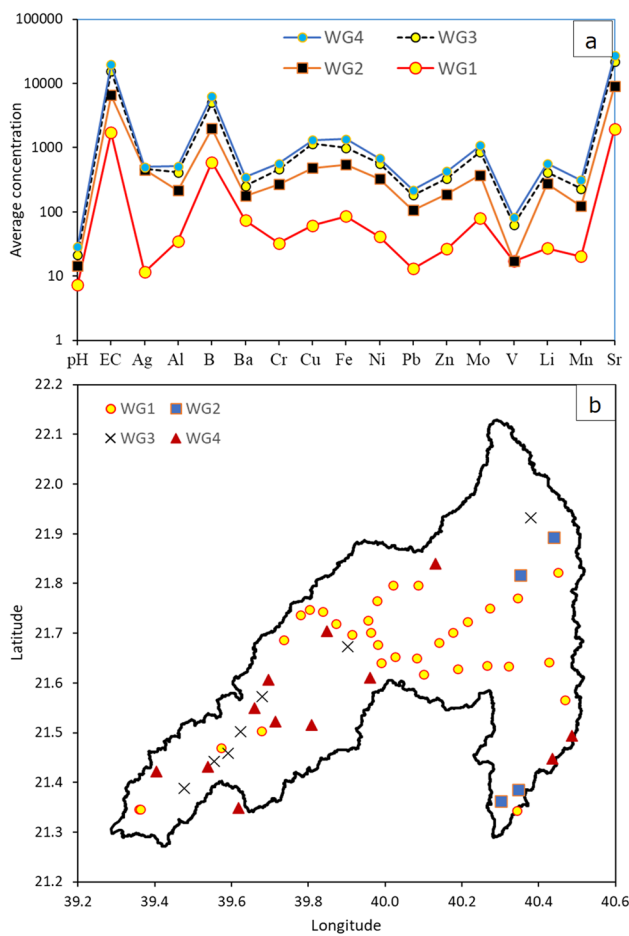


Fig. 7 The average values of pH, EC ($\mu\text{S}/\text{cm}$) and trace metals ($\mu\text{g}/\text{l}$) in HCA groups (a) and their spatial distribution (b) in the study site

In cluster WG3, seven samples (13%) are associated, and EC ranged from $6320 \mu\text{S}/\text{cm}$ to $11,580 \mu\text{S}/\text{cm}$ (mean $9107 \mu\text{S}/\text{cm}$) (Table 7). High salinity is noticed in these samples compared to other clusters and these wells are lies in the downstream region (Table 7; Fig. 7). In WG3, the average concentration of Al, B, Cu, Mo, V, Mn and Sr in the groundwater is higher than in other clusters. The average concentrations of V, Cu and Mo show significant variation and enrichment in these samples compared to other clusters. However, the variation in the average concentrations of Al, Fe and Mn between WG2 and WG3 is not significant (Fig. 7). This observation justifies that the enrichment of trace metals in the WG3 cluster wells is not due to mineral weathering alone, whereas other factors, namely evaporation, irrigation return flow and evaporite dissolution, also accumulated the metals in these wells. Hence, the water chemistry in this cluster is predominantly affected by evaporation, and evaporite dissolution followed by mineral weathering (Esmaeili et al. 2018; Barzegar et al. 2019).

Human health risk assessment

Human health risk assessment (HRA) was computed to evaluate the potential health risk due to the oral ingestion of metal-polluted groundwater for adults and children in the study area. The hazard quotient (HQ_{oral}) for each metal as well as the hazard index (HI) was calculated in this study. Figure 2 depicts the percentage of samples that surpassed the recommended value ($HQ > 1$) based on each metal. In the case of Al, all the samples surpassed the recommended limit for both adults and children. Similarly, based on the percentage of samples that exceeded the limit, the metals follow the following decreasing trend: $\text{Al} > \text{Li} > \text{Mo} > \text{Cr} > \text{Cu} > \text{Ag} > \text{Pb} > \text{Sr} > \text{Ni} = \text{B} = \text{V}$ (adults) and $\text{Al} > \text{Mo} > \text{Li} > \text{Cu} = \text{Cr} > \text{Pb} > \text{Ag} > \text{Sr} > \text{B} = \text{Ni} > \text{V}$ (children). Metals, namely Ba, Fe, Mn and Zn, have $HQ_{\text{oral}} < 1$ in all the samples.

In the study area, HI computed for adults ranged from 3 to 105 with an average of 18.8 and for children, it varied from 4 to 142 with a mean value of 25.4, respectively (Table 4). The HI values suggest that none of the samples are suitable ($HI > 1$) for drinking, which causes potential non-carcinogenic health risks to the consumer. Further, children are highly vulnerable compared to adults in the study site. Hence, the groundwater should be treated before going to supply to the local inhabitants.

Conclusions

In the Wadi Fatimah basin, there is a large variation in the salinity in the groundwater and extreme salinity is noticed in the downstream wells; however, a few wells in the upstream region also have high salinity in the groundwater. The spatial distribution pattern of trace metals also depicts a similar trend in this basin. Trace metal concentrations HPI and C_d implied that none of the samples are suitable for drinking due to the high metal load. Extreme pollution is observed by the metals, namely Li (100%), Ni (98%), Pb (86%) and B (78%), and it is in the decreasing order of $\text{Li} > \text{Ni} > \text{Pb} > \text{B} > \text{Mo} > \text{Cr} > \text{Al} > \text{Fe} = \text{Mn} > \text{V} > \text{Sr} > \text{Ag} > \text{Cu}$. Thus, the groundwater needs proper treatment before going to supply for any application.

PCA resulted in three PCs (85% of total variance) and PC1 (57% of total variance) shows the high loading of Al, Mn, Fe, EC, B and Sr which justifies the role of mixed sources, namely mineral weathering (weathering of aluminium silicates and Fe and Mn oxides/hydroxides), evaporation, irrigation return flow and evaporite dissolution. The PC2 (17%, Ag and Li) explains the impact of long storage and evaporation along with mineral weathering, and the highest positive score is recorded in the northern and southern regions. PC3 (11%, Ba, V and -pH) justified

the geogenic origin and the factor score depicts the higher values in the central part of the study area.

R-mode HCA rendered three major clusters, namely VG1, VG2 and VG3. VG1 justifies the role of rock-water interaction on water chemistry whereas VG2 indicates the predominant influences of evaporation, irrigation return flow and evaporite dissolution. Metals in VG3 imply the impact of geogenic origin in this aquifer. Q-mode HCA resulted in 4 clusters and samples in WG3 and WG2 are extremely polluted compared to other clusters. Groundwater samples in WG1 (58%) are less mineralized, and the water chemistry is governed by the mineral dissolution. In WG4 (22%), groundwater is also affected by geogenic sources; however, the enhancement of EC and metals in these wells indicates the impact of evaporation. Groundwater samples in WG2 (7%) are highly mineralized due to long storage, mineral weathering and evaporation. In WG3 (13%), groundwater shows very high salinity (EC = 6320–11,580 $\mu\text{S}/\text{cm}$) and metal load owing to the impact of irrigation return flow, evaporation and evaporite dissolution followed by mineral weathering.

Human health risk due to the oral ingestion of metal-polluted water was assessed using HQ_{oral} for each metal and hazard index, which reveals that none of them is suitable ($\text{HI} > 1$) for drinking and causes potential non-carcinogenic health risks to the consumer. Further, children are highly vulnerable compared to adults in the study site. Hence, a mitigation plan should be imposed by local municipalities and policymakers to ensure a good quality water supply to the local inhabitants. The integrated approach employed in this study can be useful to assess aquifer contamination in any region.

Supplementary Information The online version contains supplementary material available at <https://doi.org/10.1007/s13201-023-01921-6>.

Acknowledgements The authors extend their appreciation to the Deputyship for Research & Innovation, Ministry of Education in Saudi Arabia for funding this research work through the project number IFPRC-122-123-2020 and King Abdulaziz University, DSR, Jeddah, Saudi Arabia.

Funding This work was funded by the Deputyship for Research & Innovation, Ministry of Education in Saudi Arabia through the project number IFPRC-122-123-2020 and King Abdulaziz University, DSR, Jeddah, Saudi Arabia.

Data availability All data are provided as tables and figures.

Declarations

Conflict of interest The authors declare that they have no competing interests.

Ethical approval Not applicable.

Consent to participate Not applicable.

Consent to publish Not applicable.

Open Access This article is licensed under a Creative Commons Attribution 4.0 International License, which permits use, sharing, adaptation, distribution and reproduction in any medium or format, as long as you give appropriate credit to the original author(s) and the source, provide a link to the Creative Commons licence, and indicate if changes were made. The images or other third party material in this article are included in the article's Creative Commons licence, unless indicated otherwise in a credit line to the material. If material is not included in the article's Creative Commons licence and your intended use is not permitted by statutory regulation or exceeds the permitted use, you will need to obtain permission directly from the copyright holder. To view a copy of this licence, visit <http://creativecommons.org/licenses/by/4.0/>.

References

- Abiye T, Leshomo J (2014) Metal enrichment in the groundwater of the arid environment in South Africa. *Environ Earth Sci* 72:4587–4598. <https://doi.org/10.1007/s12665-014-3356-9>
- Ahmed AH, Rayaleh WE, Zghibi A, Ouddane B (2017) Assessment of chemical quality of groundwater in coastal volcano sedimentary aquifer of Djibouti, Horn of Africa. *J Afr Earth Sci* 131:284–300. <https://doi.org/10.1016/j.jafrearsci.2017.04.010>
- Aiuppa A, Allard P, D'Alessandro W, Michel A, Parello F, Treuil M, Valenza M (2000) Mobility and fluxes of major, minor and trace metals during basalt weathering and groundwater transport at Mt. Etna volcano (Sicily). *Geochim Cosmochim Acta* 64:1827–1841. [https://doi.org/10.1016/s0016-7037\(00\)00345-8](https://doi.org/10.1016/s0016-7037(00)00345-8)
- Al-Bagawi AH, Mansour D, Aljabri SAM (2021) Contaminations assessment of some trace metals in agricultural soil and irrigation water analysis at Hail region Saudi Arabia. *J Optoelectron Biomed Mater* 13:127–136
- Alfaifi H, El-Sorogy AS, Qaysi S, Kahal A, Almadani S, Alshehri F, Zaidi FK (2021) Evaluation of heavy metal contamination and groundwater quality along the red sea coast, southern Saudi Arabia. *Mar Pollut Bull.* <https://doi.org/10.1016/j.marpolbul.2021.111975>
- Al-Hobaib AS, Al-Jaseem QK, Baioumy HM, Ahmed AH (2013) Heavy metals concentrations and usability of groundwater at Mahd Adh Dhahab gold mine, Saudi Arabia. *Arab J Geosci* 6:259–270. <https://doi.org/10.1007/s12517-011-0344-1>
- Alqahtani FZ, DaifAllah SY, Alaryan YF, Elkhaleefa AM, Brima EI (2020) Assessment of major and trace elements in drinking groundwater in Bisha area, Saudi Arabia. *J Chem* 2020:5265634. <https://doi.org/10.1155/2020/5265634>
- Al-Shanti AMS (2009) Mineral deposits of the Kingdom of Saudi Arabia. Scientific Publishing Center, King Abdulaziz University, Jeddah, Saudi Arabia
- Alshehri F, Almadani S, El-Sorogy AS, Alwaqani E, Alfaifi HJ, Alharbi T (2021) Influence of seawater intrusion and heavy metals contamination on groundwater quality, red sea coast Saudi Arabia. *Mar Pollut Bull.* <https://doi.org/10.1016/j.marpolbul.2021.112094>
- Alshehri F, Zaidi FK, Alzahrani H (2022) Hydrochemical characterization of geothermal and non-geothermal waters from Wadi Fatima, western Saudi Arabia. *J King Saud University Sci* 34:101717. <https://doi.org/10.1016/j.jksus.2021.101717>
- Alshikh A (2011) Analysis of heavy metals and organic pollutants of ground water samples of South Saudi. *Life Sci J* 8:438–441
- Alyamani MS (2007) Effects of cesspool systems on groundwater quality of shallow bedrock aquifers in the recharge area of Wadi Fatimah, Western Arabian Shield, Saudi Arabia. *J Environ Hydrol* 15:1–11

- Alyamani MS, Hussein MT (1995) Hydrochemical study of groundwater in recharge area, Wadi Fatimah basin, Saudi Arabia. *GeoJournal* 37:81–89. <https://doi.org/10.1007/BF00814887>
- APHA (2017) Standard methods for the examination of water and wastewater. American Public Health Association, American Water Works Association, Water Environment Federation, Washington, DC, 23rd edition
- Arslan S, Yucel C, Calli SS, Celik M (2017) Assessment of heavy metal pollution in the groundwater of the northern Develi closed basin, Kayseri, Turkey. *Bull Environ Contam Toxicol* 99:244–252. <https://doi.org/10.1007/s00128-017-2119-1>
- ATSDR (2020) Draft toxicological profile for several trace elements. US Dept. Health Human Services, Agency for Toxic Substances and Disease Registry (ATSDR), Atlanta, GA, USA
- Backman B, Bodiš D, Lahermo P, Rapant S, Tarvainen T (1998) Application of a groundwater contamination index in Finland and Slovakia. *Environ Geol* 36:55–64. <https://doi.org/10.1007/s002540050320>
- Badr NBE, El-Fiky AA, Mostafa AR, Al-Mur BA (2009) Metal pollution records in core sediments of some red sea coastal areas, kingdom of Saudi Arabia. *Environ Monit Assess* 155:509–526. <https://doi.org/10.1007/s10661-008-0452-x>
- Bamoussa AO, El Maghraby M (2016) Groundwater characterization and quality assessment, and sources of pollution in Madinah Saudi Arabia. *Arab J Geosci* 9:536. <https://doi.org/10.1007/s12517-016-2554-z>
- Barzegar R, Asghari Moghaddam A, Soltani S, Fijani E, Tziritis E, Kazemian N (2019) Heavy Metal(loid)s in the groundwater of Shabestar area (NW Iran): source identification and health risk assessment. *Expo Health* 11:251–265. <https://doi.org/10.1007/s12403-017-0267-5>
- Basahi JM, Masoud MHZ, Rajmohan N (2018) Effect of flash flood on trace metal pollution in the groundwater - Wadi Baysh Basin, western Saudi Arabia. *J Afr Earth Sc* 147:338–351. <https://doi.org/10.1016/j.jafrearsci.2018.06.032>
- Caritat P, Danilova S, Jøger Ø, Reimann C, Storrø G, (1998) Groundwater composition near the nickel—copper smelting industry on the Kola Peninsula, central Barents Region (NW Russia and NE Norway). *J Hydrol* 208:92–107. [https://doi.org/10.1016/S0022-1694\(98\)00147-4](https://doi.org/10.1016/S0022-1694(98)00147-4)
- Edet AE, Offiong OE (2002) Evaluation of water quality pollution indices for heavy metal contamination monitoring. a study case from Akpabuyo-Odukpani area, Lower Cross River Basin (southeastern Nigeria). *GeoJournal* 57:295–304. <https://doi.org/10.1023/B:GEJO.0000007250.92458.de>
- Esmaeili S, Moghaddam AA, Barzegar R, Tziritis E (2018) Multivariate statistics and hydrogeochemical modeling for source identification of major elements and heavy metals in the groundwater of Qareh-Ziaeddin plain NW Iran. *Arab J Geosci* 11:14. <https://doi.org/10.1007/s12517-017-3317-1>
- GAE (2005) Geochemical Atlas of Europe, Part 1: Background Information, Methodology and Maps.
- Güler C, Thyne GD, McCray JE, Turner KA (2002) Evaluation of graphical and multivariate statistical methods for classification of water chemistry data. *Hydrogeol J* 10:455–474. <https://doi.org/10.1007/s10040-002-0196-6>
- Hamimi Z, Matsah M, El-Shafei M, El-Fakharani A, Shujoon A, Al-Gabali M (2012) Wadi Fatima thin-skinned foreland FAT belt: a post amalgamation marine basin in the Arabian Shield. *Open J Geology* 2:271–293. <https://doi.org/10.4236/ojg.2012.24027>
- Hem JD (1985) Study and Interpretation of the Chemical Characteristics of Natural Water. 3rd Edition, US Geological Survey Water-Supply Paper 2254, University of Virginia, Charlottesville, 263 p
- Kadam A, Wagh V, Umrikar B, Sankhua R (2019) An implication of boron and fluoride contamination and its exposure risk in groundwater resources in semi-arid region. *Environment, Development and Sustainability, Western India*. <https://doi.org/10.1007/s10668-019-00527-w>
- Kaiser HF (1960) The application of electronic computers to factor analysis. *Educ Psychol Measur* 20:141–151
- Lezzaik K, Milewski A (2018) A quantitative assessment of groundwater resources in the Middle East and North Africa region. *Hydrogeol J* 26:251–266. <https://doi.org/10.1007/s10040-017-1646-5>
- Lima AT, Safar Z, Loch JPG (2014) Evaporation as the transport mechanism of metals in arid regions. *Chemosphere* 111:638–647. <https://doi.org/10.1016/j.chemosphere.2014.05.027>
- Long X, Liu F, Zhou X, Pi J, Yin W, Li F, Huang S, Ma F (2021) Estimation of spatial distribution and health risk by arsenic and heavy metals in shallow groundwater around Dongting Lake plain using GIS mapping. *Chemosphere* 269:128698. <https://doi.org/10.1016/j.chemosphere.2020.128698>
- Massey HF, Barnhisel RI (1972) Copper, Nickel and zinc released from acid coal mine spoil materials of eastern Kentucky. *Soil Science* 113:207–212
- Masoud MHZ, Rajmohan N, Basahi JM, Niyazi BAM (2022) Application of water quality indices and health risk models in the arid coastal aquifer. *Environmental Science and Pollution Research, Southern Saudi Arabia*. <https://doi.org/10.1007/s11356-022-20835-5>
- Mielke JE (1979) Composition of the Earth's crust and distribution of the elements. In: Siegel FR (Ed), Review of Research on Modern Problems in Geochemistry. UNESCO, Paris, pp 13–37
- Mohan SV, Nithila P, Reddy SJ (1996) Estimation of heavy metals in drinking water and development of heavy metal pollution index. *J Environ Sci Health Part A Environ Sci Eng Toxicol* 31:283–289. <https://doi.org/10.1080/10934529609376357>
- Mthembu PP, Elumalai V, Brindha K, Li P (2020) Hydrogeochemical processes and trace metal contamination in groundwater: impact on human health in the Maputaland coastal Aquifer, South Africa. *Expo Health* 12:403–426. <https://doi.org/10.1007/s12403-020-00369-2>
- Narsimha A, Rajitha S (2018) Spatial distribution and seasonal variation in fluoride enrichment in groundwater and its associated human health risk assessment in Telangana State, South India. *Hum Ecol Risk Assess Int J* 24:2119–2132. <https://doi.org/10.1080/10807039.2018.1438176>
- Nouri J, Mahvi AH, Jahed GR, Babaei AA (2008) Regional distribution pattern of groundwater heavy metals resulting from agricultural activities. *Environ Geol* 55:1337–1343. <https://doi.org/10.1007/s00254-007-1081-3>
- Osta ME, Niyazi B, Masoud M (2022) Groundwater evolution and vulnerability in semi-arid regions using modeling and GIS tools for sustainable development: case study of Wadi Fatimah Saudi Arabia. *Environ Earth Sci* 81:248. <https://doi.org/10.1007/s12665-022-10374-0>
- Palmucci W, Rusi S, Di Curzio D (2016) Mobilisation processes responsible for iron and manganese contamination of groundwater in central Adriatic Italy. *Environ Sci Pollut Res* 23:11790–11805. <https://doi.org/10.1007/s11356-016-6371-4>
- Panda B, Chidambaram S, Thilagavathi R, Ganesh N, Prasanna MV, Vasudevan U (2020) Source governed trace metal anomalies in groundwater of foothill aquifer and its health effect. *Appl Water Sci* 10:173. <https://doi.org/10.1007/s13201-020-01253-9>
- Prasanna MV, Praveena SM, Chidambaram S, Nagarajan R, Elayaraja A (2012) Evaluation of water quality pollution indices for heavy metal contamination monitoring: a case study from Curtin Lake, Miri city, East Malaysia. *Environ Earth Sci* 67:1987–2001. <https://doi.org/10.1007/s12665-012-1639-6>
- Rajmohan N, Prathapar SA, Jayaprakash M, Nagarajan R (2014) Vertical distribution of heavy metals in soil profile in a seasonally waterlogging agriculture field in Eastern Ganges Basin.

- Environ Monit Assess 186:5411–5427. <https://doi.org/10.1007/s10661-014-3790-x>
- Rajmohan N, Patel N, Singh G, Amarasinghe UA (2017) Hydrochemical evaluation and identification of geochemical processes in the shallow and deep wells in the Ramganga Sub-Basin, India. *Environ Sci Pollut Res* 24:21459–21475. <https://doi.org/10.1007/s11356-017-9704-z>
- Rajmohan N, Niazi BAM, Masoud MHZ (2019) Evaluation of a brackish groundwater resource in the Wadi Al-Lusub basin Western Saudi Arabia. *Environ Earth Sci* 78:451. <https://doi.org/10.1007/s12665-019-8441-7>
- Rajmohan N, Nagarajan R, Jayaprakash M, Prathapar SA (2020) The impact of seasonal waterlogging on the depth-wise distribution of major and trace metals in the soils of the eastern Ganges basin. *CATENA* 189:104510. <https://doi.org/10.1016/j.catena.2020.104510>
- Rajmohan N, Masoud MHZ, Niyazi BAM (2021) Assessment of groundwater quality and associated health risk in the arid environment, Western Saudi Arabia. *Environ Sci Pollut Res* 28:9628–9646. <https://doi.org/10.1007/s11356-020-11383-x>
- Rajmohan N, Niyazi BAM, Masoud MHZ (2022) Trace metals pollution, distribution and associated health risks in the arid coastal aquifer, Hada Al-Sham and its vicinities Saudi Arabia. *Chemosphere* 297:134246. <https://doi.org/10.1016/j.chemosphere.2022.134246>
- Reimann C, Bjorvatn K, Frengstad B, Melaku Z, Tekle-Haimanot R, Siewers U (2003) Drinking water quality in the Ethiopian section of the East African Rift Valley I—data and health aspects. *Sci Total Environ* 311:65–80. [https://doi.org/10.1016/S0048-9697\(03\)00137-2](https://doi.org/10.1016/S0048-9697(03)00137-2)
- Ren X, Li P, He X, Su F, Elumalai V (2021) Hydrogeochemical processes affecting groundwater chemistry in the central part of the Guanzhong basin, China. *Arch Environ Contam Toxicol* 80:74–91. <https://doi.org/10.1007/s00244-020-00772-5>
- Salminen R, Batista MJ et al (2005) *Geochemical Atlas of Europe. Part 1—Background Information, Methodology and Maps*.
- Samadder SR, Prabhakar R, Khan D, Kishan D, Chauhan MS (2017) Analysis of the contaminants released from municipal solid waste landfill site: a case study. *Sci Total Environ* 580:593–601. <https://doi.org/10.1016/j.scitotenv.2016.12.003>
- Şen Z, Al-Harithy S, As-Sefry S, Almazroui M (2017) Aridity and risk calculations in Saudi Arabian Wadis: Wadi Fatimah case. *Earth Syst Environ* 1:26. <https://doi.org/10.1007/s41748-017-0030-x>
- Senior LA, Sloto RA (2006) Arsenic, Boron, and Fluoride in Ground Water in and Near Diabase Intrusions, Newark Basin, Southeastern Pennsylvania. U.S. Geological Survey Scientific Investigations, pp 105
- Sharaf MAM (2013) Major elements hydrochemistry and groundwater quality of Wadi Fatimah, West Central Arabian Shield, Saudi Arabia. *Arab J Geosci* 6:2633–2653. <https://doi.org/10.1007/s12517-012-0544-3>
- Taylor BE, Foord EE, Friedrichsen H (1979) Stable isotope and fluid inclusion studies of gem-bearing granitic pegmatite-aplite dikes, San Diego Co., California. *Contrib Mineral Petrol* 68:187–205
- Ure AM, Berrow ML (1982) The elemental constituents of soils. In: Bowen HJM (ed) *Environmental chemistry*, vol 2. The Royal Society of Chemistry, pp 94–204
- USEPA (2012) Edition of the drinking water standards and health advisories. EPA, Washington
- USEPA (1989) Risk assessment guidance for superfund, volume 1: human health evaluation manual (part A). United States Environmental Protection Agency, Office of Emergency and Remedial Response, Washington DC
- USEPA (1993) Reference dose (RfD): description and use in health risk assessments. US Environmental Protection Agency, Office of Water, Washington, , DC. <http://www.epa.gov/iris/rfd.htm>
- USEPA (2011) Exposure factors handbook: 2011 Edition (Final Report). U.S. Environmental Protection Agency, Washington, DC, EPA/600/R-09/052F, 2011
- USEPA (2014) Human health evaluation manual, supplemental guidance: Update of standard default exposure factors, OSWER Directive 9200.1–120. United States Environmental Protection Agency, Washington, DC
- USEPA (2019) Integrated risk information system (IRIS). U.S. EPA, Washington, DC. <https://www.epa.gov/iris>
- Usman UA, Yusoff I, Raoov M, Hodgkinson J (2020) Trace metals geochemistry for health assessment coupled with adsorption remediation method for the groundwater of Lorong Serai 4, Hulu Langat, west coast of Peninsular Malaysia. *Environ Geochem Health* 42:3079–3099. <https://doi.org/10.1007/s10653-020-00543-0>
- Ward JH (1963) Hierarchical grouping to optimize an objective function. *J Am Stat Assoc* 58:236–244. <https://doi.org/10.1080/01621459.1963.10500845>
- Wen X, Lu J, Wu J, Lin Y, Luo Y (2019) Influence of coastal groundwater salinization on the distribution and risks of heavy metals. *Sci Total Environ* 652:267–277. <https://doi.org/10.1016/j.scitotenv.2018.10.250>
- WHO (2001) Vanadium pentoxide and other inorganic vanadium compounds. Concise International Chemical Assessment Document 29. Geneva
- WHO (2003a) Boron in drinking-water. background document for development of WHO guidelines for drinking-water quality. World Health Organization, Geneva. WHO/SDE/WSH/03.04/54 .
- WHO (2003b) Lead in drinking-water. background document for development of WHO guidelines for drinking-water quality. World Health Organization, Geneva. WHO/SDE/WSH/03.04/09/Rev/1.
- WHO (2003c) Aluminium in drinking-water. background document for development of WHO Guidelines for drinking-water quality. World Health Organization, Geneva. WHO/SDE/WSH/03.04/53
- WHO (2003d) Chromium in Drinking-water. background document for development of WHO guidelines for drinking-water quality. World Health Organization, Geneva. WHO/SDE/WSH/03.04/04
- WHO (2017) Guidelines for drinking water quality: fourth edition incorporating the first addendum. World Health Organization, Geneva
- Zaidi FK, Nazzal Y, Jafri MK, Naeem M, Ahmed I (2015) Reverse ion exchange as a major process controlling the groundwater chemistry in an arid environment: a case study from northwestern Saudi Arabia. *Environ Monit Assess* 187:607. <https://doi.org/10.1007/s10661-015-4828-4>

Publisher's Note Springer Nature remains neutral with regard to jurisdictional claims in published maps and institutional affiliations.